

Omega-P, Inc.

199 Whitney Ave., Suite 200, New Haven, CT 06511

20-MW MAGNICON FOR ILC

FINAL TECHNICAL REPORT

Phase I SBIR Grant #DE-FG02-05ER 84396

TABLE OF CONTENTS

I.	INTRODUCTION	p. 2
II.	TECHNICAL APPROACH FOR PHASE I R&D	4
III.	ANTICIPATED PUBLIC BENEFITS	6
IV.	RESULTS OF PHASE I R&D	8
	IVa. Technical objectives of Phase I	8
	IVb. Work Plan for Phase I	8
	Task 1. Electron gun	9
	Task 2. Magnetic system	12
	Task 3. Beam dynamics simulations	13
	Task 4. Design of output cavity	16
	Task 5. Output couples and output waveguides	20
	Task 6. Beam collector	21
V.	CONCLUSIONS	23
VI.	REFERENCES	24

Principal Investigator: J. L. Hirshfield
jay@omega-p.com

November, 2006

I. INTRODUCTION

Under Topic 37b in the DoE 2005 SBIR Program Solicitation, Phase I proposals were sought "...to develop new concepts, high-power RF components and instrumentation to be used in producing high peak power in narrow band, low duty-cycle, and low pulse repetition frequency (approximately 0.1 to 1 kHz) pulsed RF amplifiers. The principal application is to future large electron/positron linear colliders. Potential electrical efficiencies greater than 45 percent are considered essential..." Omega-P, Inc. submitted a proposal in response, entitled "20-MW Magnicon for ILC," and was awarded the Phase I grant DE-FG02-05 ER84368, with the same title. The overall goal of this R&D program was to develop a magnicon amplifier at 1.3 GHz with peak power output of 20 MW for the future International Linear Collider ILC [1].

In the present ILC Baseline Configuration [2], the two main linear accelerators are each to be built from roughly 10,000 one-meter long, 9-cell superconducting cavities operating at 1.3 GHz. Eight of these cavities are to be installed in a common cryomodule, and three cryomodules are to be driven by each 10-MW RF source. The accelerating gradient is to be 31.5 MeV/m for a c.m. energy in the first stage of 0.5 TeV (later upgraded to 0.8 TeV). However, the RF system must provide 35 MeV/m in the first stage, and 40 MeV/m in the upgrade. The RF-power is to be generated by some 600 (1200) klystrons. The RF pulse length is ~1.5 ms, which includes the beam pulse length of 1000 μ s, and the cavity fill time of 500 μ s. The repetition rate is 5 Hz. Discussion of ILC parameters is ongoing, so some may change.

Three versions of 10 MW multibeam klystrons (MBK's) have so far been built as candidate RF sources for ILC. The status of these tubes is summarized (as of March 24, 2006) in the ILC Latest Official Version of the Baseline Configuration Document (BCD), Main Linacs Section, in which the following statement appears:

"The 10 MW Multi-Beam Klystrons (MBK's) being developed by Thales, CPI and Toshiba are the baseline choice. The basic tube design appears to be robust while alternative approaches have not been fully designed nor are currently funded to be developed. At worst, if the MBK's do not meet availability requirements, the commercial, single-beam, 5 MW tube from Thales could be used (it has been the 'work-horse' for L-band testing at DESY and FNAL). Although it is less efficient (42% vs 60-65%), this tube has been in service for over 30 years with good availability."

It can be pointed out that reduction in RF source efficiency from 65% to 42% would represent a 55% increase in electrical power demand for the RF system, which would significantly alter the economic basis upon which ILC is to be "marketed."

Comments of knowledgeable specialists on the utility of these MBK's for ILC are accessible in the online record. For example, at the 2005 SLAC DoE Program Review, Chris Adolfsen stated that MBK's "...are not fully proven." Lutz Lilje of DESY reported in March 2006 at LCWS06 in Bangalore on the ILC main linac design status that 10 MW, 1.3 GHz MBK's "...currently do not have a robust tube design...nor are yet built for horizontal mounting." And in a widely-circulated February 19, 2006 letter of resignation from FNAL, G. William Foster states that "...after 10 years of development the ILC main linac does not have a klystron that works." These remarks cannot help but raise doubts in the minds of objective observers, and indicate that any reasonable alternative to the MBK for ILC deserves be developed at least to the prototype stage, to allow realistic evaluation and comparison with the

MBK. As an example of this, the SLAC Klystron Department is developing a 10-MW L-band sheet beam klystron, to lower cost (as compared with “expensive” MBK’s), and as a backup “...if the multi-beam program falters.” [C. Adolfsen] The L-band magnicon proposed here is another alternative, but one which has the advantage of being based upon twenty years of experience in development and operation of magnicons in other frequency domains [3,4,5,6].

Still, without presuming any basic flaw in the concept of a 10-MW MBK for ILC, it should be instructive to list points that support development of a 20-MW magnicon as an alternative to the MBK, together with points that tend to favor the MBK. Points that appear to favor development of a 20-MW L-band magnicon for ILC include the following:

1. The number of magnicons would be half of what is needed when MBK’s are used, resulting in fewer sockets, fewer mains power distribution points, and a simplified modulator and RF control infrastructure.
2. The RF distribution system will only be slightly modified from that using MBK’s, as each magnicon will have four 5-MW outputs, *versus* two 5-MW outputs for each MBK.
3. The number of modulators will be cut in half, although each will need to supply ~220 kW, rather than 120 kW.
4. The production cost for each $P = 20$ -MW magnicon should be about 40% lower than that for two 10-MW MBK’s, if each tube’s cost scales classically, i.e., in proportion to \sqrt{P} . But savings might be even greater, since each magnicon could have fewer parts than each MBK. If each MBK were to cost \$200k, the capital savings could amount to about \$100M, using 600 magnicons instead of 1200 MBK’s.
5. The magnicon is predicted to have an efficiency of up to 75%, instead of 67% for the MBK. This could lead to a present value of ac mains power savings over 15 years of about \$160M, based on electricity cost of \$0.10/kW-hr.
6. The peak RF electric field in the magnicon would be only 66 kV/cm, as compared to 115 kV/cm in an MBK, giving greater reliability and longer lifetime for magnicons.
7. High-power circulators are not needed for tube protection when magnicons are used, leading to significant cost savings (~25% of the RF distribution cost) and RF circuit simplifications.
5. Power variation with voltage V , i.e. $(dP/P)/(dV/V)$, is calculated to be 0.42 for the magnicon, *versus* measured values of 1.8 for the Toshiba MBK, and 2.5 for CPI. This leads to less stringent modulator voltage stability specifications for the magnicon.

In contrast, several compelling points tend to favor the MBK, including the following:

1. The MBK has a lower beam voltage than the magnicon (117 kV vs 300 kV). For a 300 kV magnicon, the pulse transformer iron yoke and oil tank will be ~2.6 times bigger in volume than for the MBK. The voltage pulse leading edge could be longer. Nevertheless, the modulator and pulse transformer for each magnicon could probably be built for roughly the same cost as two modulators and pulse transformers for MBK’s.
2. It is probably not possible to develop a 300 kV cable to connect the magnicon to a remotely sited pulse transformer, as compared with a 117 kV cable for the MBK. Thus

the pulse transformer for the magnicon must be in the service tunnel with the tube, rather than above ground. This adds complexity in the tunnel, but eliminates altogether the need for a high-voltage cable.

3. The RF cavity chain in the magnicon is 180-200 cm long, *versus* 150 cm for Thales MBK. The magnicon gun is 47 cm high, *versus* 35 cm for MBK. The Thales beam collector is only 65 cm long, *versus* 190 cm for the preliminary design collector for the magnicon. However, this preliminary length for the magnicon collector is highly conservative and will be reduced in subsequent designs, especially if the collector is not required to dissipate the full beam power without RF drive.

4.. The x-ray dose with a 300 kV magnicon is greater than for a 117 kV MBK. But if the pulse transformer for magnicon is in the tunnel, this difference could be immaterial.

The above polemic is of course an insufficient basis upon which justify investment and effort needed to develop a 20-MW 1.3 GHz magnicon for ILC, notwithstanding the desirability for an alternative to the mainline MBK's. Rather, it is the scientific merits for the magnicon presented in this proposal that Omega-P believes do provide the needed justification.

II. TECHNICAL APPROACH FOR PHASE I R&D

The magnicon [7] is a microwave amplifier tube that combines the scanning-beam synchronism of the gyrocon [8] with a cyclotron resonant interaction in the output cavity. The transverse momentum that drives the output cavity interaction is generated in a series of deflection cavities that operate in synchronously rotating TM_{110} modes. The input cavity acts upon a small diameter solid electron beam, where rotating RF fields of an externally-driven TM_{110} mode convert a small fraction of the beam axial momentum into transverse momentum (Larmor motion), directed across the applied axial DC magnetic field. The beam then transits a sequence of gain cavities, where the transverse beam momentum induces amplified RF fields that further deflect the beam, producing a progressively higher fraction of transverse momentum. The RF fields in each deflection cavity rotate synchronously with the externally-driven RF fields of the drive cavity. Unlike the gain cavities of a klystron, those of the magnicon are not used to create bunching, but rather to amplify the transverse motion of the beam. Because all of the cavities contain synchronously rotating modes, electron motion is synchronous with the phase of the RF fields in each of the deflection cavities. As a result of the phase-synchronous transverse deflection of the electron beam as a whole, the beam electrons entering the output cavity execute Larmor motion whose entry point and guiding center rotate in space about the cavity axis at the drive frequency. In the output cavity, the beam drives a cyclotron-resonant interaction with a synchronously rotating TM_{m10} mode, at the m^{th} harmonic of the drive frequency, which extracts power principally by reducing the transverse beam momentum. In order to obtain high efficiency, electrons should have roughly equal transverse to longitudinal momenta in the output cavity. As will be discussed below, an alternative output circuit has been studied during Phase I in which a TE_{111} -mode cavity is used in place of the TM_{110} mode. It will shown that this strategy leads to much lower RF surface fields in the output cavity for a fixed power output, with increased resilience to breakdown which should lead to improved tube reliability and longer lifetime.

Several versions of the magnicon have been built, from the decimeter to the millimeter wavelength domains, operating in the first, second and third harmonic modes. The first magnicon (at the first harmonic, or fundamental) was built and tested in 1985 [3]. A power of 2.6 MW was obtained at 915 MHz with a pulse length of 30 μ sec and electronic efficiency of 85%. The device was successfully tested with absorbing loads, but also with a resonant accelerating structure, without use of a ferrite circulator [9]. This showed that reflections from a resonant load need not lead to excitation of spurious modes of oscillation in a magnicon, nor that damage to the tube will result. The high efficiency obtained with the 915 MHz magnicon, albeit with relatively low power and short pulse length, provides confidence that the development program proposed here for a 1.3 GHz magnicon for ILC should meet with success.

Other magnicons at wavelengths from decimeter to millimeter ranges for have also been developed. A second magnicon is a frequency doubler (or 2nd harmonic amplifier), operating at a frequency of 7 GHz [10,11]. This tube has demonstrated experimentally an output power of 55 MW, an efficiency of 56%, and a gain of \sim 70 dB in 1 μ sec pulses, in very good agreement with simulation results [4,12]. Another frequency-doubling magnicon amplifier [5] at the NLC frequency of 11.424 GHz has been designed and built in a collaboration between Omega-P, Inc. and Naval Research Laboratory (NRL). The tube is designed to produce \sim 60 MW at 60% efficiency and 59 dB gain, using a 470 kV, 220 A, 2 mm-diameter beam. At present, the tube is conditioned up to power level of 25 MW for 0.2 μ sec pulse widths. Operation of this latter magnicon has established a research facility located at NRL as only the second laboratory in the USA, after SLAC, where high-power microwave development at the X-band frequency can take place. A high power third-harmonic magnicon at 34.272 GHz has been designed and built as a microwave source to develop RF technology for a future multi-TeV electron-positron linear collider. After preliminary RF conditioning, this tube produces an output power of over 30 MW in 0.5 μ s pulses, with a gain of 54 dB [13]. These preliminary results already constitute record values for a millimeter-wave accelerator-class amplifier. While the second and third harmonic magnicon amplifier concepts were introduced in order to achieve high power in the cm- and mm-wave ranges, the first harmonic amplifier has higher efficiency and smaller size than harmonic versions; this can be especially critical at decimeter wave lengths.

A diagram of a 20 MW, 1.3 GHz first-harmonic magnicon design for ILC is shown in Fig. 1, and preliminary design parameters are presented in Table I. The electron gun injects a small diameter pencil beam into a chain of cavities forming the RF system. The deflection system consists of a drive cavity and six gain cavities to provide the required deflection angle at the output cavity. The external magnetic field provides both beam focusing and coupling between the electrons and the RF fields in the cavities. The scanning beam rotates at the frequency of the drive signal, then enters the output cavity and emits radiation by interacting with the TM_{110} (or perhaps TE_{111}) mode. All cavities of the RF deflection system oscillate in the circularly polarized TM_{110} mode at 1.3 GHz. The proposed magnicon amplifier will operate with a 300 kV, 100 A electron beam to meet the requirements for operation in ILC, namely 20 MW peak output power with a 1.5 ms pulse duration, and a 5 Hz repetition rate. It should be noted that the collector depicted in Fig. 1 was designed conservatively, to be capable of dissipating the full beam power at a 10 Hz repetition rate *without* RF drive power. The final design is to be for 5 Hz rate *with* RF drive, since alternate pulse operation of an XFEL is not considered part of ILC. With a 5 Hz repetition rate, and for operation only with RF, the

collector would need to dissipate only about 20 kW average power, and would thus be much smaller than that shown in Fig. 1.

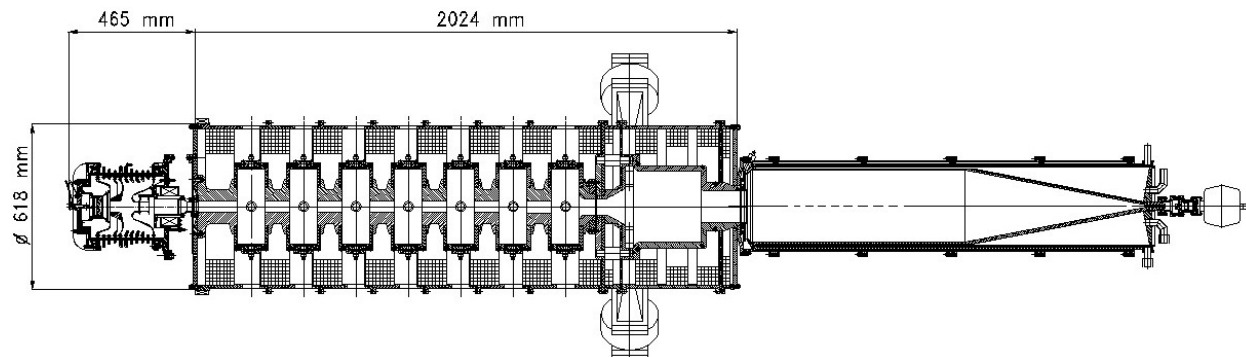


Fig. 1. Diagram of the proposed 20-MW, 1.3 GHz magnicon.

Table I. Preliminary design parameters of 20 MW, 1.3 GHz magnicon amplifier.

operating frequency, MHz	1300
maximum output peak power, MW	22.5
maximum average power, kW	180
pulse duration, msec	1.6
repetition rate, Hz	5
efficiency, %	~70-75
gain, dB	>44
FWHM bandwidth, MHz	~2
beam power, MW	30
beam voltage, kV	300
beam current, A	100
beam perveance, $A/V^{3/2}$	0.61×10^{-6}

III. ANTICIPATED PUBLIC BENEFITS

Advancement in high-energy physics has, in the years since WWII, brought enormous practical benefit to the US public in general, and to the US scientific community in particular. Widely-dispersed benefits include fast integrated-circuit electronics, accelerators for radiotherapy and industrial processing, nuclear power, and the internet. For the scientific community, achievements include many discoveries on the fundamental nature of matter and on the origin of the universe. But vexing questions persist, including the nature of dark matter, the origin of mass, extra dimensions, and the need "...to illuminate the pathway to the underlying simplicity of the universe."* High-energy physics research has been carried out by large international research groups, that include many scientists trained in the US, using facilities built and operated in the US, thus evincing great pride and prestige among Americans. This positive climate attracted many of brightest young Americans and foreign scholars to high-energy physics and created a scientific work force in the US that is envied and emulated

*R. L. Orbach, in oral testimony before the US House Committee on Appropriations, 3/15/05.

by advanced societies the world over. The curtain on this era in the US could be falling as other countries may be taking the lead in high-energy physics, including the European Community that is now building LHC at CERN in Geneva (with partial US support, it should be said). The international high-energy physics community has pronounced a TeV-scale lepton collider ILC as the next step in its search for a fundamental understanding of Nature. In August 2004, ICFA recommended that, for ILC, a superconducting collider should be built at an initial c-o-m energy of 0.5 TeV, with a possible future upgrade to 0.8 TeV. The competing US/Japan design NLC/GLC that came in behind the superconducting option, in ICFA's view, embodies a room-temperature pair of 10-km microwave-driven linacs, that would be designed to also reach a c-o-m energy of 0.5 TeV, but with possible future upgrade to 1.5 TeV.

Benefits to the international scientific community and to the public at large can be anticipated from results of future basic research in high-energy physics, as has been amply demonstrated from such research in the past. It is widely recognized that future large accelerators are to be international projects, including the 0.5–1.0 TeV International Linear Collider ILC. The specific justification for efforts to develop a next-generation 0.5 – 1.0 TeV electron-positron collider has been thoroughly studied and justified in a number of international forums [14,15], wherein it was concluded that the best approach towards successful realization of a 0.5 – 1.0 TeV collider was through use of super-conducting rf technology, operated at L-band, i.e. at a frequency of 1300 MHz. Efforts over the past five years have been directed at development of 10 MW multi-beam klystrons to meet this need [16,17,18]. Approximately 600 of these tubes would be required for the 0.5 TeV collider, and 1200 tubes for the 1.0 TeV upgrade. Results of the Phase I R&D reported here offer strong computational evidence for the possibility of designing and operating a magnicon at twice the MBK power level, namely at 20 MW; other parameters of the 20 MW magnicon would satisfy ILC requirements, although the predicted magnicon efficiency of 75%, is about 10% higher than for the MBK, offering the attractive potential of significant savings in electrical power costs during the lifetime of the machine. The evident simplification and cost savings attending a reduction by a factor-of-two in numbers of large rf amplifiers and associated components would be a decided advantage in favor of the 20 MW magnicon. Furthermore, since magnicons have been shown capable of operating into resonant loads without excitation of spurious modes, it could be possible to configure ILC using magnicons without high-power circulators, thus providing another source of capital savings. But detailed cost savings will only be known once a successful prototype of the magnicon has been designed, built, and operated. Indeed, realization of that prototype is the ultimate goal of the effort proposed here.

In a letter enclosed in the Phase I proposal, Dr. George Caryotakis, then head of the Klystron/Microwave Department at SLAC, considered potential benefits of the magnicon for ILC and wrote:

“...It seems to me that the basic nature of the tube itself should make it well suited for development at L-band. The parameters that your preliminary simulations have given would represent an intriguing match to the needs of ILC, in that one of your tubes would replace two multi-beam klystrons of the type now under development by Thales, CPI, and Toshiba. From what I know of Omega-P's experience with other magnicons, I can see no insurmountable obstacle to prevent success with the L-band tube....”

IV. RESULTS OF PHASE I R&D

IVa. Phase I Technical Objectives*

The overall goal of the Phase I program was to develop a self-consistent design of a 1.3 GHz pulsed magnicon for use in ILC. Design has been performed for a 20 MW first harmonic amplifier with efficiency of 70-75%, 1.5 msec pulse duration, and a repetition rate of 5 Hz. The effort has included detailed analytical studies and numerical simulations of a complete magnicon amplifier, which includes the electron gun, RF structure, magnet system and collector. A strategy was evolved for further development of the tube, assuming that sufficient resources would be made available for this undertaking.

IVb. Phase I Work Plan*

Major issues that were addressed during Phase I included the following:

Task 1: Design a 30 MW triple anode gun to produce a 300 kV, 100 A beam. The current density on the cathode is not to exceed 2.7 A/cm^2 , and the maximum electric field on the focus electrodes is to be about 50 kV/cm. An optimal design will be selected for matching the beam into the deflecting system of the magnicon with an axial guide magnetic field of about 930 G. Analysis of the gun assembly tolerances is also to be carried out.

Task 2: Conceptual design will be performed of the magnicon magnetic system in order to achieve optimal field profile so as to provide maximum tube efficiency. The magnetic system should also provide optimal beam matching with the electron gun, and optimal beam dispersion in the collector.

Task 3: Optimization of the beam dynamics will be conducted in order to meet the tube design parameters. Beam dynamics simulations are to be carried out both for the steady-state regime and the transient process in the magnicon. Stability analysis of operating regimes is to be performed, as well as analysis of influence of space charge effects on the tube parameters. Analysis of the tolerances of the cavity's frequency and position are to be performed also.

Task 4: Design of the output cavity will be performed so as to insure absence of current interception in the RF system in all possible regimes of tube operation.

Task 5: Optimization will be carried out of the output couplers and output waveguides, with either two or four outputs.

Task 6: Conceptual design will be conducted of a beam collector capable of operating with a beam having peak power of 30 MW (i.e., up to 50 kJ/pulse).

Task 7: A strategy will evolve during Phase I for further development of the tube.

*The statement of technical objectives and tasks for Phase I are paraphrased directly from the Phase I proposal. The change in pulse repetition rate from 10 down to 5 Hz is for consistency with ILC needs; design changes to the tube from this are insignificant, except for the collector.

Results of work on these tasks will be described below.

Task 1. Electron Gun.

Due to the long pulse, the acceptable electric field in the gun must be relatively low. For pulse lengths longer than about 1.0 msec, an empirical relation for the high voltage breakdown threshold is given by $E_s V_e < 800 \text{ kV}^2/\text{mm}$, where E_s is surface electric field on the electrode at lower potential and V_e is the voltage between two electrodes [19]. This requirement represents a challenge in the gun design which can be overcome by using a multi-gap (multi-anode) gun concept. In the proposed magnicon, the beam parameters are: beam voltage of 300 kV and beam current of 100 A. To provide these parameters with a pulse-width of about 2 msec, a triple-anode gun with a spherical cathode 8 cm in diameter has been designed. A layout of the electrode configuration for the gun and sample electron trajectories are shown in Fig. 8. The maximum cathode loading doesn't exceed $2.7 \text{ A}/\text{cm}^2$, which allows one to expect good cathode longevity of $\sim 100,000$ hours according to [20] (see Figure 9). Current density distribution over the cathode surface is shown in Figure 10.

In the present gun design, $E_s = 51 \text{ kV}/\text{cm}$ on the focus electrode and $E_s V_e = 510 \text{ kV}^2/\text{mm}$ between the first anode and the focus electrode. On the first anode $E_s = 45 \text{ kV}/\text{cm}$ and $E_s V_e = 450 \text{ kV}^2/\text{mm}$ between the two anodes. On the second anode $E_s = 50 \text{ kV}/\text{cm}$ and $E_s V_e = 500 \text{ kV}^2/\text{mm}$ between the two anodes. These values are comfortably below the breakdown limit. Long life cathode operation can be expected with these levels of surface field in the gun [20]. Preliminary gun design parameters are listed in Table II.

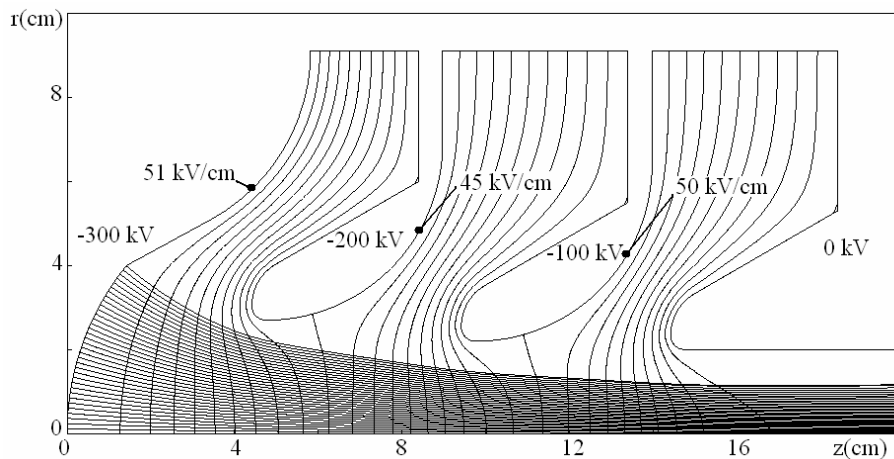


Figure 2. The triple-anode gun conceptual layout, showing trajectories, equipotential lines, potentials, and peak electric fields on the focus electrode and each intermediate anode.

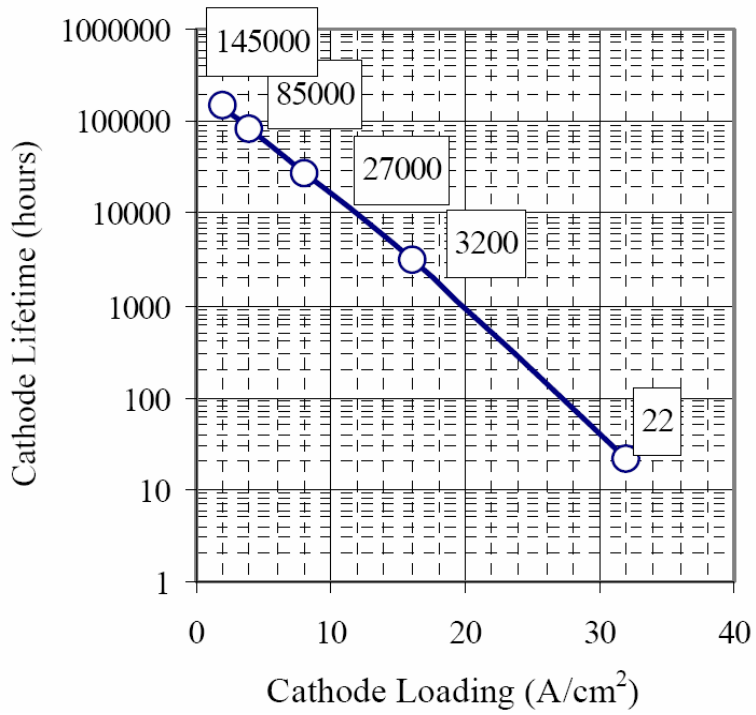


Figure 3. Semi-empirical curve showing the prediction of dispenser cathode lifetime *versus* cathode loading [20].

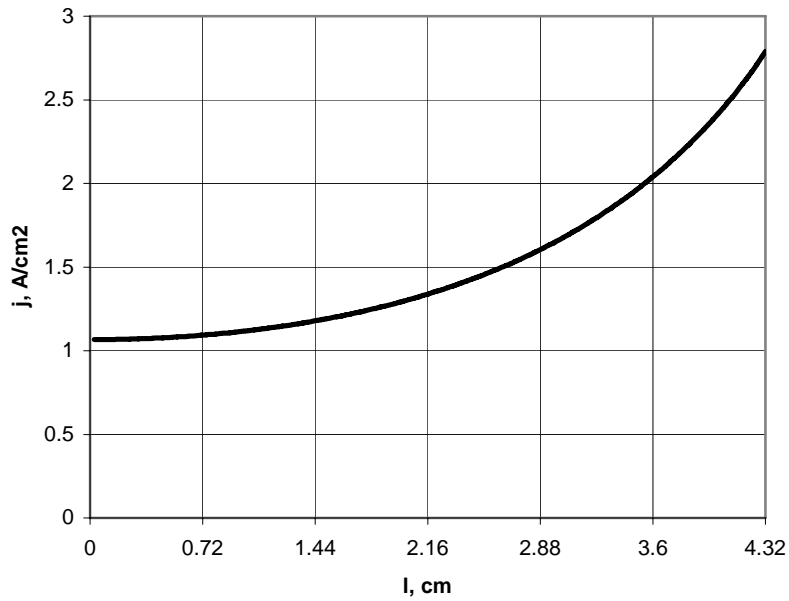


Figure 4. Current density distribution along the cathode surface for the gun design described here; $l=0$ corresponds to the cathode center.

Table II. Design parameters of the electron gun for a 20 MW, 1.3 GHz magnicon.

beam voltage, kV	300
beam current, A	100
beam power, MW	30
beam perveance, $A/V^{3/2}$	0.61×10^{-6}
pulse duration, μsec	1.6
repetition rate, Hz	5
cathode diameter, mm	80
maximum cathode loading, A/cm^2	2.7
number of anodes	3
voltage between the cathode and the 1 st anode, kV	100
maximum electric field on the focus electrode (the 1 st gap), kV/cm	51
voltage between the 1 st anode and 2 ^d anode, kV	100
maximum electric field on the 1 st anode (the 2 ^d gap), kV/cm	45
voltage between the 2 ^d anode and 3 ^d anode, kV	100
maximum electric field on the 2 ^d anode (the 3 ^d gap), kV/cm	50
electrostatic compression	11:1

A gun engineering design similar to what is required is shown in Fig. 5, except that an additional intermediate anode would be added, as introduced in the simulations so as to reduce electric fields on the electrodes well into safe operating regimes for ms pulse lengths.

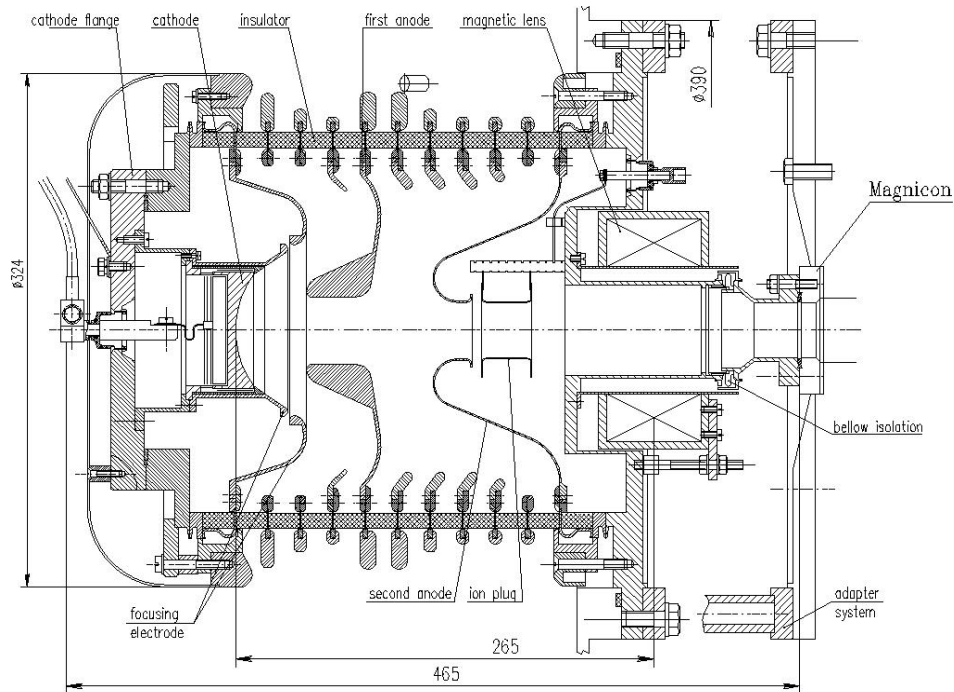


Figure 5. An engineered gun design similar to that required for the 20-MW L-band magnicon.

The sectioned ceramic insulator is similar to that which has been built for the Omega-P 34 GHz magnicon gun. The insulator consists of 10 rings with an external diameter of 250

mm, having a length of 20 mm each. The uniformity of the electric field along the insulator is achieved by optimizing of the shapes of the anodes and the special intermediate electrodes attached to the insulator (see Fig. 6). The same electrodes protect the insulator from scattered electrons and photons. A set of external ~ 40 pF capacitors and 10 Mohm resistors are also included in order to ensure the uniformity of electric field gradient and prevent charge buildup. Due to a relatively low filament power of 350 W, no special means for cooling of the insulator and anodes is required. The field equipotential lines are shown in Fig. 7. The uniformity of electric field along the insulator is better than $\pm 10\%$. The electron gun is attached to the magnicon with an adapter coil that provides accurate beam alignment. The matching lens is positioned inside of the adapter, and cannot be removed without breaking vacuum; it is therefore made of special wire that allows for high temperature bakout.

Prior tests of the dispenser cathode at the vendor's site indicate that, under ion bombardment, the diffusion of active elements on the cathode surface to recover destroyed spots is not sufficient even with the elevation of the cathode temperature. For short pulse operation, this problem is not too significant; but for long-pulse operation of the magnicon for ILC, the vendor has decided to take a precautionary measure, namely to introduce an ion plug in the gun with a trapping potential of up to 5 kV below ground that is expected to essentially eliminate ion bombardment of the cathode. This ion plug is in evidence in Fig. 6.

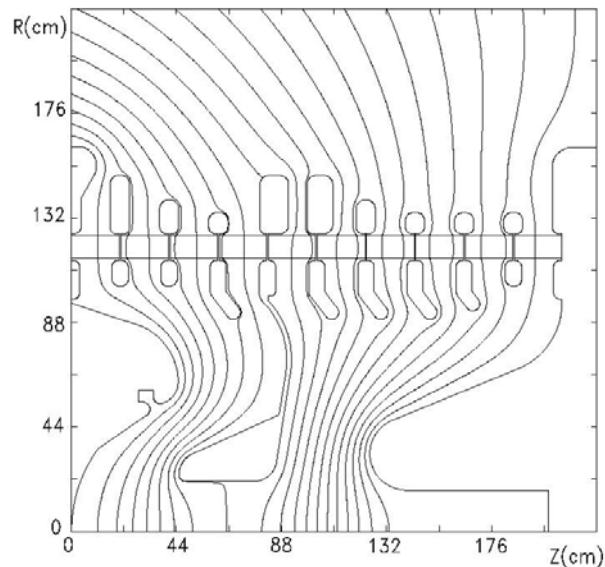


Fig. 6. Equipotential lines in the gun.

Task 2. Magnetic System.

The magnetic field profile and the magnetic circuit required to produce the profile were determined by iterative simulations to optimize magnicon performance. Iterations in field profile were coupled with iterations in cavity designs. Figure 7 shows the optimized magnetic field profile (top) and the coil configuration and iron yoke geometry to achieve this profile (bottom). For effective deflection, the magnetic field in the deflection system should be about 930 Gauss. However, in the output cavity, for efficient extraction of energy, the magnetic field

should be about 650 Gauss. This field profile is created by use of a series of coils and judiciously positioned iron pole pieces. The required levels of magnetic field are quite modest.

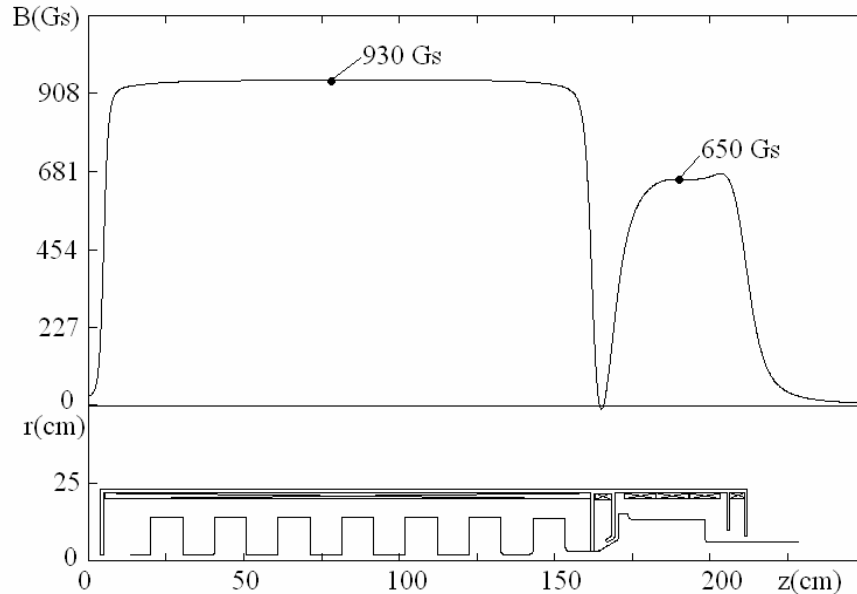


Figure 7. Required axial magnetic field profile (top), coils and iron yoke layout (bottom). Cavity chain is also shown.

Task 3. Beam Dynamics Simulations.

The shapes of the cavities are carefully designed to get high efficiency with the smallest possible magnitude of RF fields in the cavities. The maximum surface electric fields in the penultimate and output cavities do not exceed 75 kV/cm. All cavities in the deflection system are 280 mm in diameter and 100 mm long. For efficient interaction the RF electric and magnetic fields in the TM_{110} output cavity must have nearly similar profiles along the axis, as shown in Fig. 8. Such profiles were obtained by increasing the diameter of the cavity near its entrance [21] as can be seen in Fig. 8. Increase in diameter of the output cavity to 306 mm is also advantageous when using four output waveguides and windows, as is now planned at the high power level, and as suggested in [22].

In Fig. 9 and 10 are shown the results of steady-state trajectory simulations. Figure 9 shows the beam particle's energies along the tube, while Figure 10 shows the magnitude of radial excursions for the beam trajectories and the profile of the cavities. One can see in Figure 9 that the deceleration is relatively uniform, and that the beam loses a substantial part of its energy (>70% on average). The beam trajectories seen in Figure 10 show that there is no current interception on the tube walls. The absence of current interception was proven experimentally in different tested versions of magnicons [3,4,5,6].

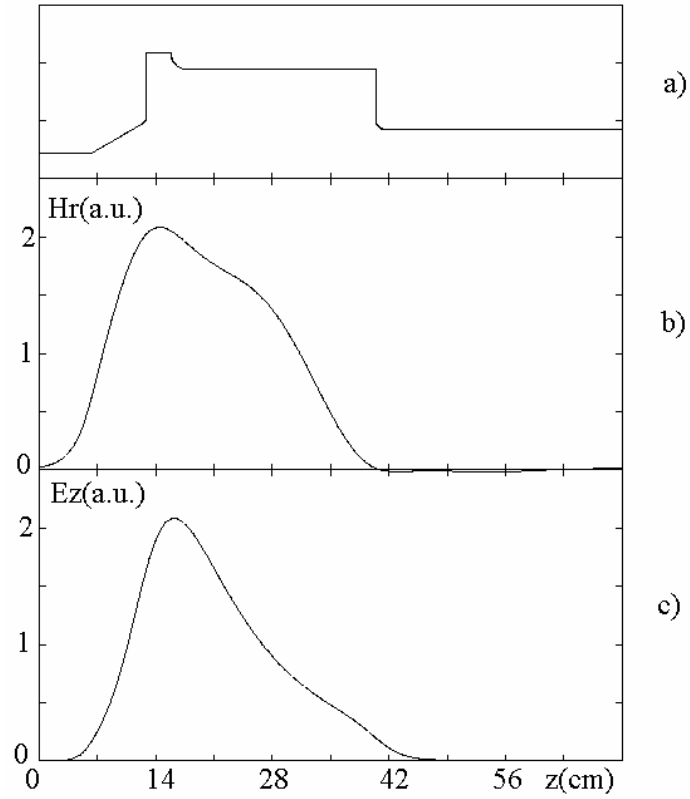


Figure 8. (a) The TM_{110} output cavity layout, (b) transverse magnetic field and (c) longitudinal electric field distribution along the cavity axis at a radius of 20 mm.

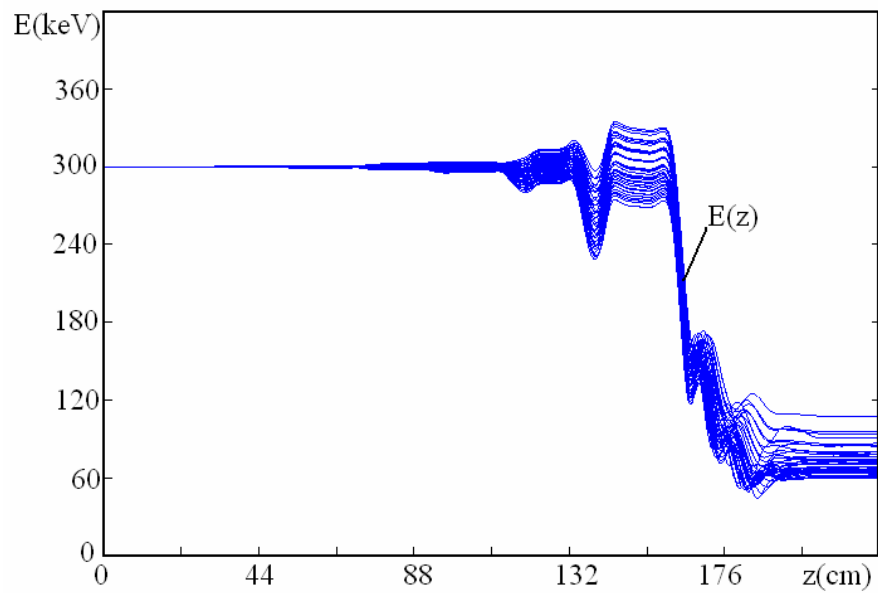


Figure 9. Energies $E(z)$ of beam particles in transit through the magnicon cavities.

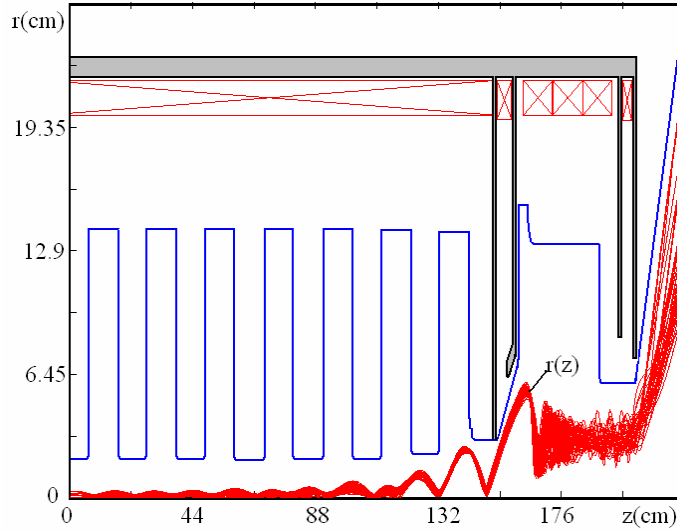


Figure 10. The outline of the RF cavities, magnetic system, and radial coordinates of beam electrons r , all as functions of coordinate z along the axis of the tube.

Confirmation that the build-up of gain the magnicon will be stable is provided by time-dependent simulations of transient processes, results of which are shown in Figure 11. One can see that the transient process is smooth, and that the build-up time for steady oscillations is about $0.8 \mu\text{sec}$. The calculated dependence of the drive curve, i.e. output power *vs.* input power, is shown in Figure 12. The drive curve is monotonic, indicating that the tube operates stably within the full range of output power, up to about 22.5 MW, with a margin more than 10% above the 20-MW rating for the tube. Calculated magnicon output power *vs.* drive frequency is shown in Figure 13. It indicates that the tube FWHM bandwidth is about 2 MHz.

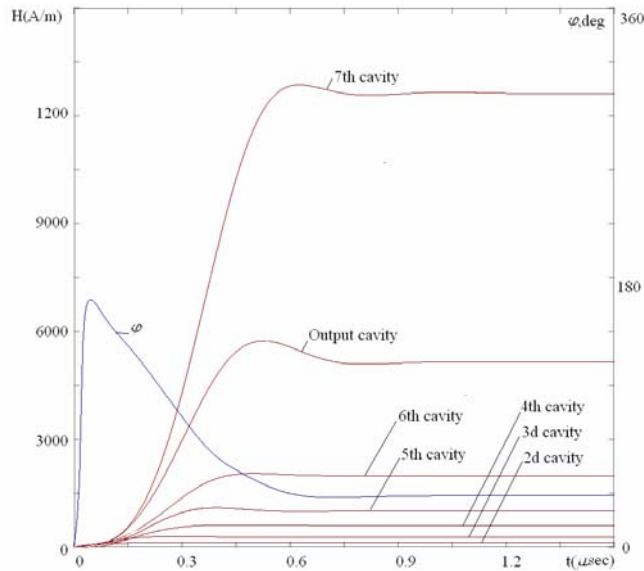


Figure 11. Example of transient processes in the magnicon. Shown are the computed RF amplitudes in the cavities and phase φ in the output cavity, as functions of time from the start of the RF pulse.

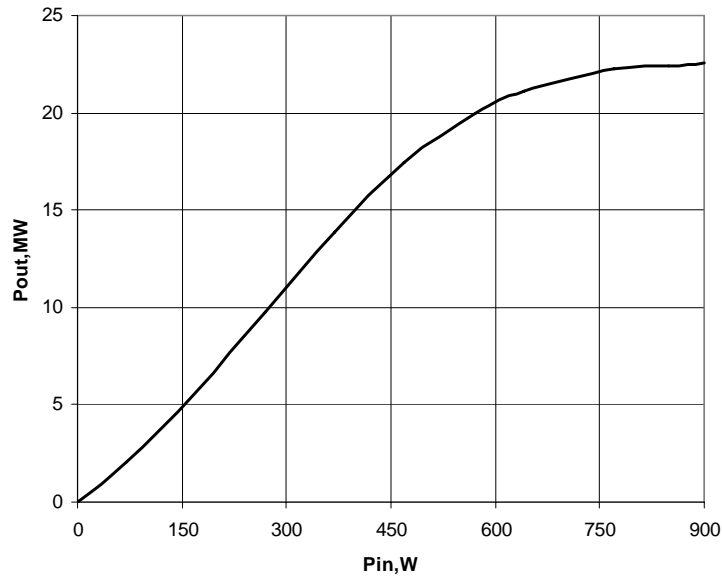


Figure 12. Output power vs. input power.
 Note that in this example the output power actually rises to greater than 22 MW.

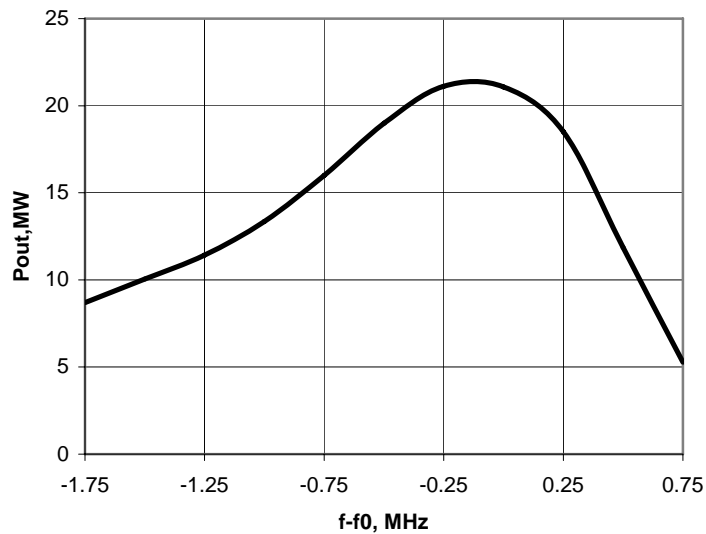


Figure 13. Output power vs. frequency, for an input power of 650 W. Peak gain is 45.2 dB.

Task 4. Design of Output Cavity.

Results shown above in Figures 7-13 are for a conventional magnicon cavity chain where, for first-harmonic (or fundamental) operation, all cavities (input, deflection/gain, and output) operate in the TM_{110} mode. During Phase I, in addition to simulation studies to optimize the TM_{110} mode output cavity for high efficiency without unduly high surface fields, a preliminary study was made of a modified magnicon in which the output cavity operates in the TE_{111} mode. In this case, the physics of energy extraction from the beam differs from that for

the TM_{110} mode. For the TE_{111} mode, azimuthal particle deceleration occurs by work done on the azimuthal RF electric field along a spiral path whose length can exceed the cavity length by a substantial factor; in the TM_{110} mode case, work is done on the axial electric field with a path length equal to the axial length of the cavity. For equal incoming deflected beam parameters and equal power output, this difference in path lengths leads to need for a much lower RF electric field magnitude in the TE_{111} mode case, with a corresponding need for a lower output cavity quality factor Q . An optimized cavity outline that was found to satisfy this requirement is shown in Figures 14 and 15.

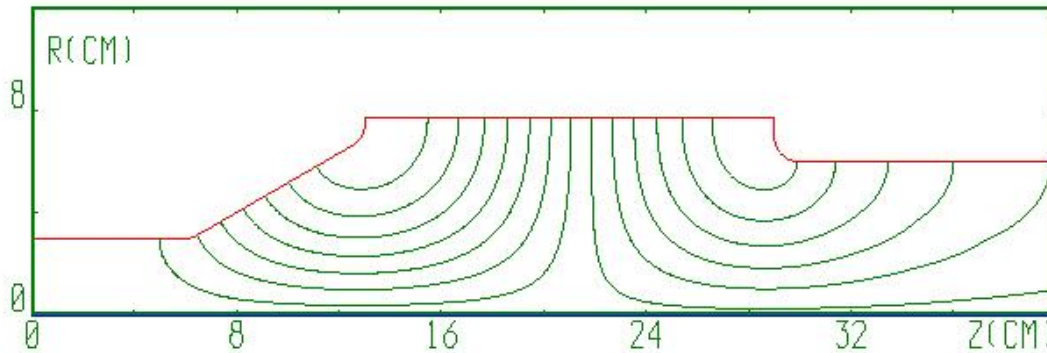


Figure 14. The TE_{111} cavity layout and “field map” (i.e., surfaces, where $rH_\phi = const$).

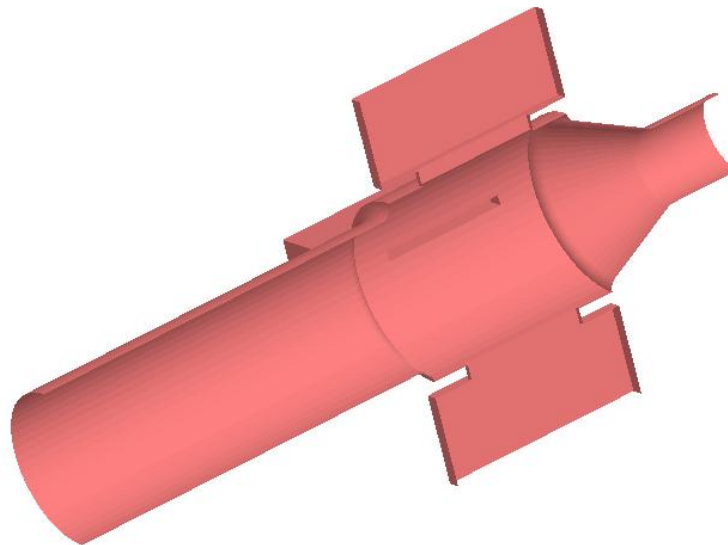


Figure 15. Cut-away drawing of TE_{111} -mode output cavity model with four output waveguides.

Comparison with Fig. 8 shows that choice of the TE_{111} mode would reduce the length of the output cavity from 38 cm to 16 cm, with a corresponding reduction in length of the overall cavity chain. Field profiles are shown in Fig. 16; amplitude reflection coefficient S_{11} as a function of frequency is shown in Fig. 17; and beam trajectories and energies in Fig. 18.

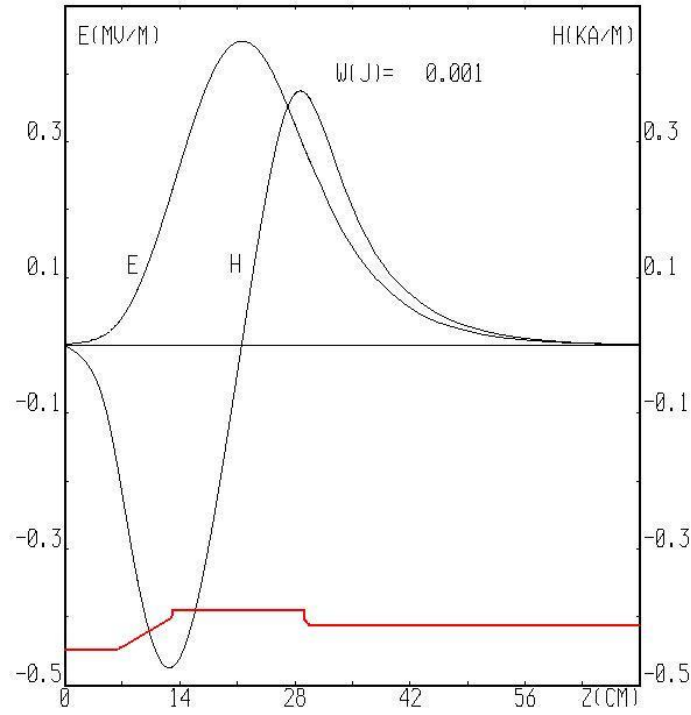


Fig. 16. The transverse electric and magnetic field profiles along the output cavity axis for the TE_{111} mode output cavity.

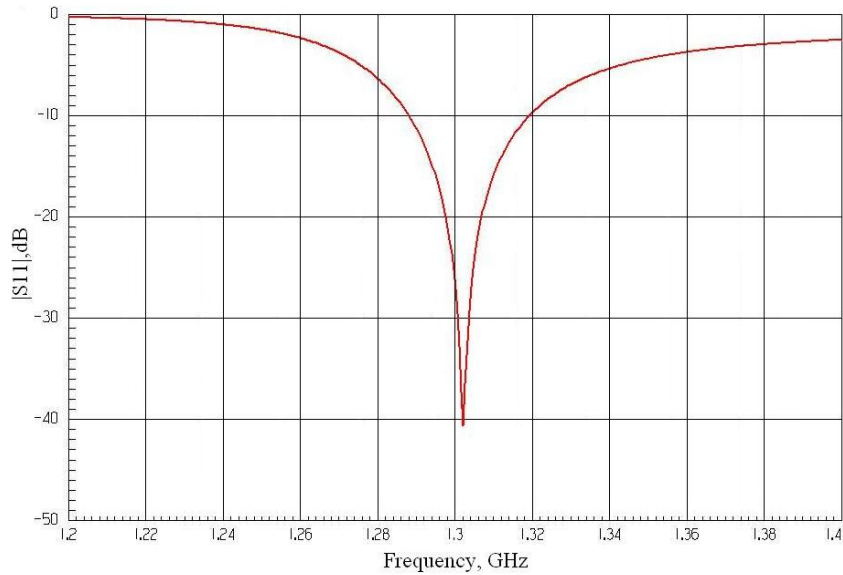


Figure 17. Relative reflected amplitude S_{11} (in dB) vs. frequency for the TE_{111} cavity of Fig. 16. As is seen, very slight adjustments are needed to lower the eigenfrequency to 1.30 GHz, but the quality factor is equal to the design value of $Q = 16$.

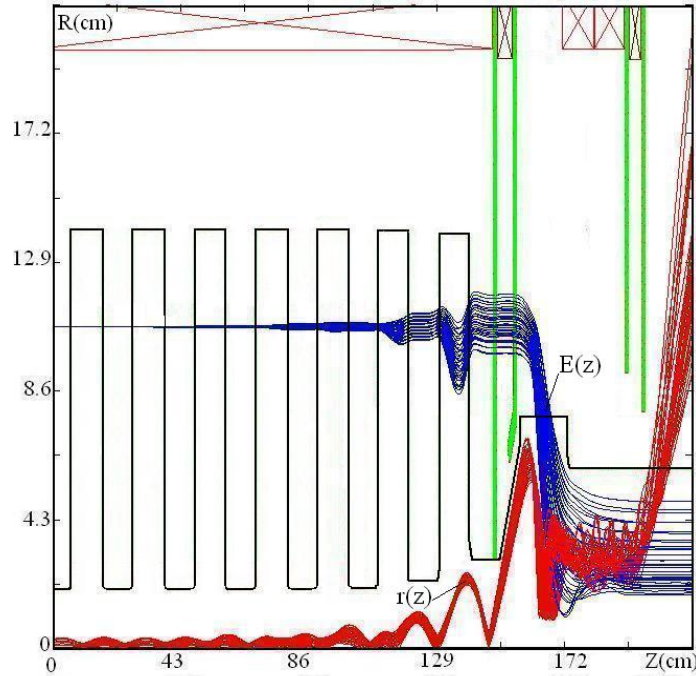


Fig. 18. Radial coordinates of the beam trajectories $r(z)$ and the particle energies $E(z)$ for the tube with a TE_{111} output cavity. The distance between the beam edge and the output cavity wall is about 5 mm. Note that the beam radius in the front end of the output cavity is bigger than the output beam tunnel radius, but is reduced near the output end of the cavity. The DC magnetic field profile for this example is very similar to that shown in Fig. 7.

Fig. 19 compares computed output power *versus* frequency, for magnicons employing TM_{110} and TE_{111} mode output cavities, while Fig. 20 compares drive curves at the frequency of peak output power. These results show that the tube performance would be virtually identical, whichever output cavity is chosen. The choice of modes may thus be made on the basis of selecting the lowest maximum surface field in the cavity, which favors the TE_{111} mode, and on the basis of optimized coupling, which is still to be fully explored. Comparative parameters are given in Tables III and IV.

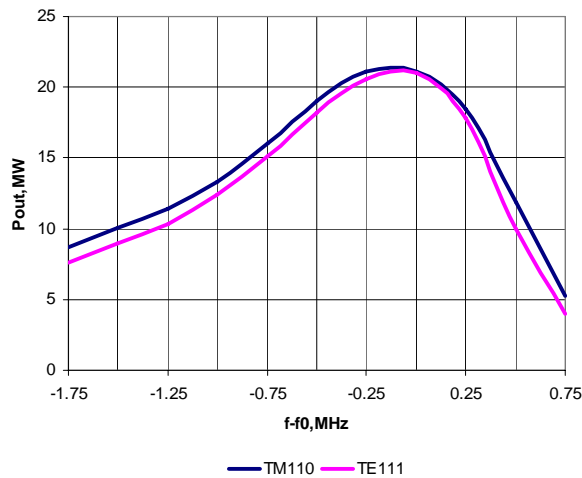


Figure 19. Output power *versus* frequency for TM_{110} and TE_{111} mode output cavities.

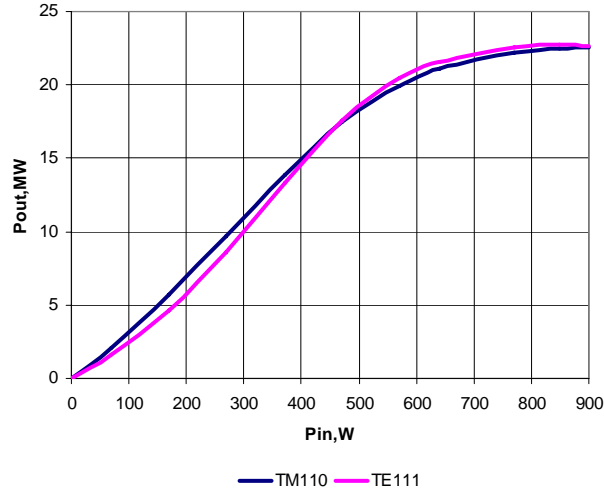


Figure 20. Drive curves for TM_{110} and TE_{111} mode output cavities.

Table III. Main parameters of magnicons with TE_{111} and TM_{110} output cavities.

	Input Power, W	Output power, MW	Efficiency,%	Gain,dB
TM_{110}	850	22.5	75.0	44
TE_{111}	850	22.7	75.7	46

Table IV. Parameters of the TE_{111} cavity vs. TM_{110} cavity (5 Hz, 1.5 msec)

	Unloaded Q	Loaded Q	Average power losses in the penultimate cavity, kW	Average power losses in the output cavity, kW	E_{\max} in the penultimate cavity, kV/cm	E_{\max} in the output cavity, kV/cm
TM_{110}	29500	90	1	0.5	66	74
TE_{111}	29400	16	1	0.1	66	16

Task 5. Output couplers and output waveguides.

The output cavities shown in Figs. 8 and 16 contains four output waveguides whose widths are identical to widths of standard WR-650 rectangular waveguide, but whose heights are reduced. Gentle height tapers, output windows, and (probably) a right-angle bend would complete the output circuit. The final disposition of the four outputs for would be perpendicular to the beam collector for TM_{110} cavity and parallel to the beam collector for TE_{111} cavity (as shown in Fig. 18), to facilitate installation of coils and pole pieces that are beyond the output cavity. Simulations of the interaction in the output cavity lead to field plots as shown in Fig. 21, for coupling that optimizes the cavity Q factor. In these diagrams, beam enters from right.

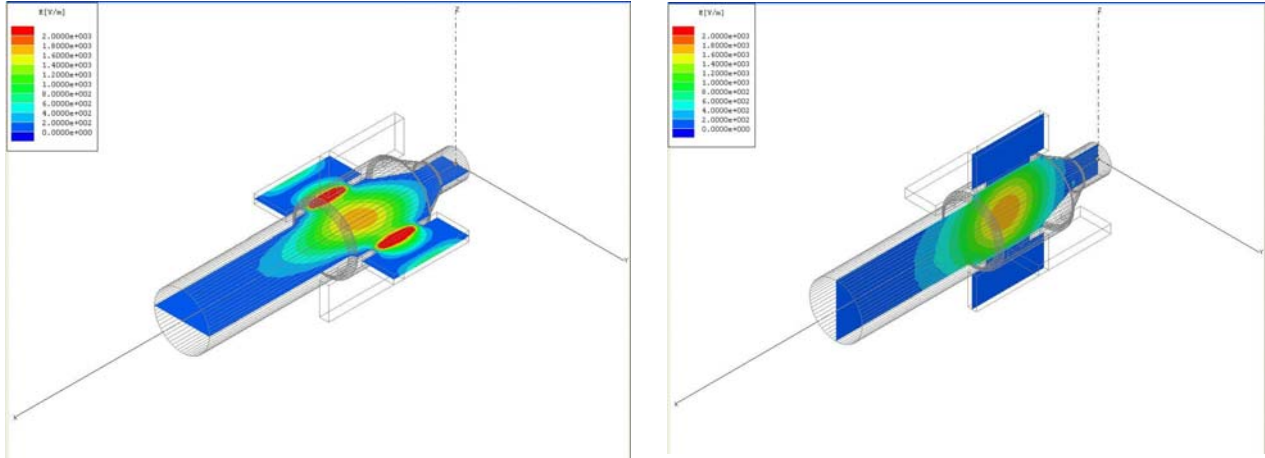


Figure 21. Field pattern in TE_{111} -mode output cavity with four output waveguides, at a phase value when the rotating cavity fields couple into two horizontal waveguides (at left), while no coupling appears in the vertical pair of waveguides (at right). One-quarter cycle later, coupling moves from horizontal to vertical waveguides.

Task 6. Beam Collector.

The output segment of the magnet system is designed so as to optimize extraction of the beam energy into RF fields of the output cavity, to avoid current interception in the drift tube leading to the collector entrance, and to prevent electron reflections from the collector from returning to the cavities. Computed electron trajectories in the collector are shown in Fig. 22 for full RF output power, and in Fig. 23 for the case of zero RF drive (and thus full beam power). These simulations are for the case of a TM_{110} mode output cavity. As described elsewhere [23], these simulations include a reliable model for elastic scattering of primary beam electrons and for the emission of up to five generations of secondary electrons.

From Fig. 22, one can see that virtually the entire beam will be collected within a length of about 80 cm, whereas without RF drive Fig. 23 shows that a 70 cm greater length will be required. This shows that the design of a collector in a production tube, where operation without RF drive can be limited or eliminated, would be quite different from the design of a collector for an experimental device. For continuous operation without RF drive, the heat to be dissipated from the collector would be four times higher than with RF drive.

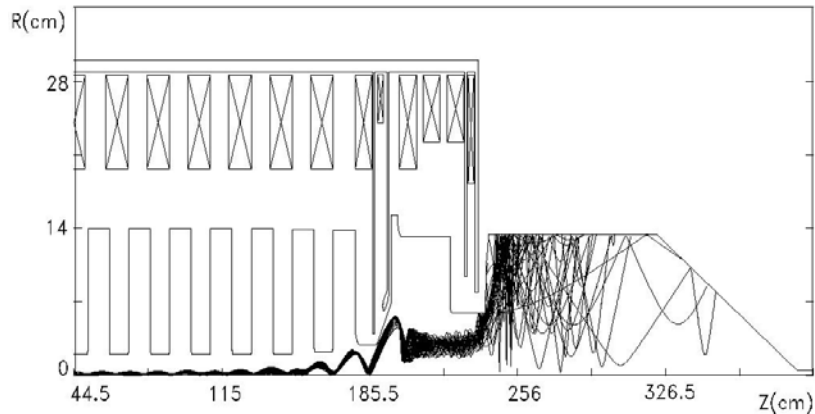


Figure 22. Projection in (r, z) plane of electron trajectories for full output power.

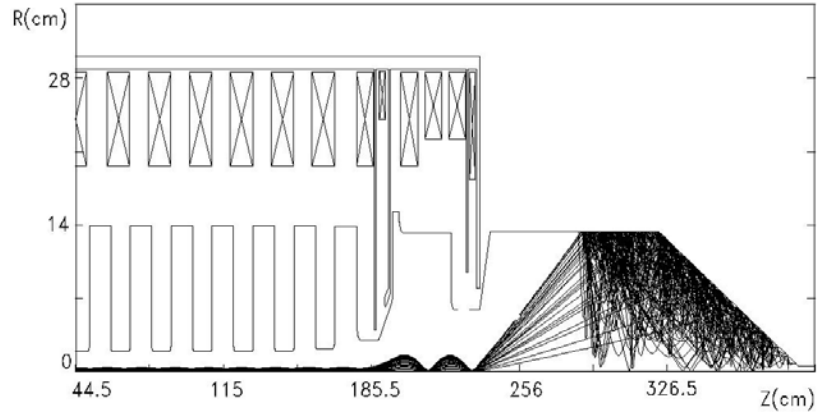


Figure 23. Projection in (r,z) plane of electron trajectories for zero drive signal.

Engineering considerations for the high-power beam collector can be illustrated by reference to Fig. 24. The main elements shown are the collector itself (1), the water jacket (2), the separator of the water flow (3), and the outer shield (4). The collector (1) would be made of OFHC copper, while the other parts (2, 3 and 4) would be made of stainless steel. To measure the beam current, the entire collector is insulated from the ground using a ceramic insulator.

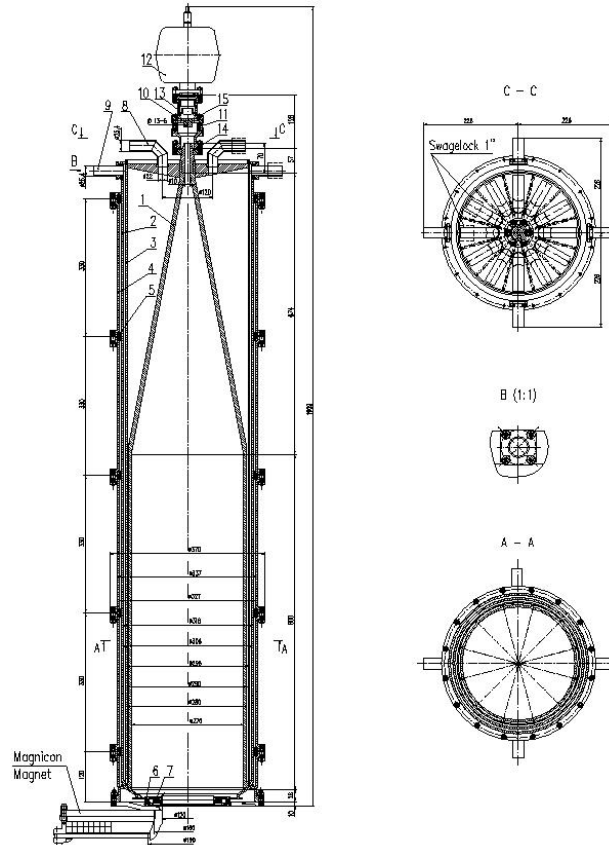


Figure 24. Example of the engineering design of a high-power magnicon beam collector, capable of dissipating the 240 kW of beam power from full pulse-width, full repetition rate operation without RF drive power. A practical collector need only operate with RF, and thus at an average power level of 60-80 kW, and would be much smaller. .

The outer shield (4) consists of five sections, mechanically attached to the output flange of the magnicon, and centered with respect to collector with the help of rings (5) made of an insulating material. This shield serves the dual function of providing mechanical strength, and of centering. It also works as a grounded shell of the insulating collector. Such a collector design allows operation of the tube in either vertical or horizontal mounting positions. The collector is connected to the magnicon structure by ceramic insulator (6) and a short bellows (7). In order to maintain azimuthal uniformity of the water cooling, the water jacket is separated into twelve sections (see A-A and C-C in Fig. 9). Each section has its own inlet water pipe (8). The coolant leaves the water jacket through four outlet pipes (9). This design allows dissipation of the full beam power of 160 kW. The required water flow is about 250 liters/min and the maximum temperature rise on the collector surface is about 130 °C with no RF drive and about 60 °C with RF drive.

In order to avoid possible damage of the collector end due to ion focusing (in case of poor vacuum and without rf drive) there is a pipe 10 mm in diameter and 70 mm long installed at the far end of the collector. Under normal operating conditions electrons do not penetrate through this pipe. But in case of ion focusing the thin central core of the beam does pass the pipe and is intersected by molybdenum target (10). This target is insulated from the collector and vacuum pump (12) by insulators (11) and (13) to allow measurement of the intersected current, thereby providing a warning of deteriorated vacuum in the collector.

V. CONCLUSIONS

Conceptual design of a 20-MW, 1.3 GHz magnicon amplifier for ILC has been described. This tube, with parameters listed in Table I, could replace two multi-beam klystrons now under development as RF sources for ILC. Advantages of the magnicon are listed in Section I of this report, and contrasted with advantages of MBK's. The magnicon described in this report could be developed and demonstrated in a collaboration involving three organizations: Omega-P, Inc., Yale University Beam Physics Laboratory, and an established industrial manufacturing firm (the "Industrial Partner") with experience in the science, engineering design, and fabrication of high-power RF tubes. Alliance with a high-power RF tube manufacturing facility is considered important in order to gain access to additional advanced high-power RF engineering expertise, to employ advanced microwave tube fabrication technologies, and to process the tube appropriately, including prolonged high-temperature vacuum oven bakeout (550 °C).

In the end, Omega-P concluded that it would not be prudent to proceed with an application for Phase II SBIR funding for this project. This decision was taken not because of any lack of confidence in the scientific and technical basis of the magnicon design outlined in this report. Rather, it was taken in view of the scant interest on the part of the ILC community to undertake development of an alternative to the MBK, coupled with that lack of funding within the limited budget of the US ILC R&D program. However, should interest and resources towards development of the 20-MW magnicon for ILC materialize in the future, Omega-P would be willing to provide its expertise within a collaboration organized along lines sketched above, to work towards a successful outcome.

VI. REFERENCES

1. The International Linear Collider. <http://www.linearcollider.org/cms/>
2. The International Linear Collider. Global Design Effort. Baseline Configuration Document, March 28, 2006,
http://www.linearcollider.org/wiki/doku.php?id=bcd:bcd_home#latest_official_version_of_bcd
3. M.M.Karliner, E.V.Kozyrev, I.G.Makarov, O.A.Nezhevenko, G.N. Ostreiko, B.Z.Persov, and G.V.Serdobintsev, "The Magnicon - An Advanced Version of the Gyrokon," *Nucl. Instrum. Methods Phys. Res. A* **269**, 459-473 (1988).
4. E.V. Kozyrev, O.A. Nezhevenko, A.A. Nikiforov, G.N. Ostreiko, G.V. Serdobintsev, S.V. Schelkunoff, V.V. Tarnetsky, V.P. Yakovlev, I.A. Zapryagaev, "Present Status on Budker INP 7 GHz Pulsed Magnicon", RF98 Workshop, Pajaro dunes, October 5-9, 1998, AIP Conference Proc. 474, Woodbury, N.Y., 1999, pp.187-194.
5. O.A. Nezhevenko, V.P. Yakovlev, J.L. Hirshfield, E.V. Kozyrev, S.H. Gold, A.W. Fliflet, and A.K. Kinkead, "Performance Of X-Band Pulsed Magnicon Amplifier," *Proc. 2003 Particle Accelerator Conf.*, Portland, May 11-16, 2003, pp.1128-1130
6. O.A. Nezhevenko, M.A. LaPointe, V.P. Yakovlev, J.L. Hirshfield, "Commissioning of the 34-GHz 45-MW Pulsed Magnicon," *IEEE Trans. Plasma Sci.*, vol.32 pp. 994-1001, June, 2004.
7. O.A. Nezhevenko, "Gyrocons and Magnicons: Microwave Generators with Circular Deflection of the Electron Beam," *IEEE Trans. Plasma Sci.* **22** pp. 765-772, Oct., 1994.
8. G.I. Budker, M.M. Karliner, I.G. Makarov, S.N. Morosov, O.A. Nezhevenko, G.N. Ostreiko, and I.A. Shekhtman, "The Gyrocon—An Efficient Relativistic High-Power VHF Generator," *Part. Accel.*, vol. 10, pp. 41–59, 1979.
9. V.E. Akimov *et al.*, "Accelerating system of the racetrack microtron", Preprint INP 89-162, Novosibirsk, 1989 (in Russian). Deposited into NTIS database.
10. O.A. Nezhevenko, *Proceeding of 1991 Particle Accelerator Conference*, San Francisco, 1991, (IEEE, Piscataway, NJ, 1992), p.2933.
11. V.E. Akimov, Yu.V. Baryshev, B.S. Estrin, M.M. Karliner, I.V. Kazarezov, E.V. Kozyrev, G.I. Kuznetsov, I.G. Makarov, O.A. Nezhevenko, G.N. Ostreiko, B.E. Persov, G.V. Serdobintsev, M.A. Tiunov, V.P. Yakovlev, and I.A. Zapryagaev. *Proceedings of 1990 European Particle Accelerator Conference*, Nice, 1990, (World Scientific, Singapore, 1991), p. 1000.
12. E.V. Kozyrev, O.A. Nezhevenko, A.A. Nikiforov, G.N. Ostreiko, B.Z. Persov, G.V. Serdobintsev, S.V. Schelkunoff, V.V. Tarnetsky, V.P. Yakovlev, I.A. Zapryagaev, "New Results of 7 GHz Pulsed Magnicon Amplifier Investigations", *Proceeding of 1998 European Particle Accelerator Conference*, Stockholm, June 22-26, 1998, p.1897.
13. O.A. Nezhevenko, V.P. Yakovlev, M.A. LaPointe, E.V. Kozyrev, S.V. Shchelkunov, and J.L. Hirshfield, "Status Of 34 GHz, 45 MW Pulsed Magnicon," *Proceeding of 2005 Particle Accelerator Conference*, Knoxville, May 16-20, 2005, p. 1922-1924.
14. International Linear Collider Technical Review Committee, 2^d Report, SLAC-R-606, SLAC, 2003.
15. Final International Technology Recommendation Panel Report, September 2004, www.fnal.gov/directorate/icfa/ITRP_Report_Final.pdf

16. A. Beunas, G. Faillon and S. Choroba, "A High Power Long Pulse High Efficiency Multi- Beam Klystron,"
http://tdserver1.fnal.gov/8gevinacPapers/Klystrons/Thales_multi_beam_Klystron_MDK2001.pdf
17. A. Balkcum, H.P. Bohlen, M. Cattelino, L.Cox, M. Cusick, S.Forrest, F. Friedlander, A. Staprans, E.L. Wright, L. Zitelli, K. Eppley, "Design and Operation of a High Power L-Band Multiple Beam Klystron," *Proceeding of 2005 Particle Accelerator Conference*, Knoxville, 2005, p.2170.
18. Y.H. Chin, S. Choroba, M. Y. Miyake, Y. Yano, "Development of Toshiba L-Band Multi-Beam Klystron for European XFEL Project," *Proceeding of 2005 Particle Accelerator Conference*, Knoxville, 2005, p. 3153.
19. High Voltage Vacuum Insulation, Edited by R.V. Latham, Acad. Press, N.Y., 1995, pp. 403-429.
20. E. Wright, A. Balkcum, H. Bohlen, *et al.*, "Development of 10-MW, L-Band Multiple-Beam Klystron For TESLA," *Proceeding of 2003 Particle Accelerator Conference*, Portland, May 11-16, 2003, pp.1144-1146.
21. A. Nezhevenko, V.P. Yakovlev, and A.K. Ganguly, "Long-Pulse 1.3GHz Magnicon", *Proceeding of 1998 European Particle Accelerator Conference*, Stockholm, June 22-26, 1998, p.1906.
22. Y.H. Chin and V. Vogel, "Simple-Minded Upgrade Paths to 800 GeV or Higher," *First ILC Workshop*, KEK, November 2004, <http://lcdev.kek.jp/ILCWS/WG1.php>.
23. V. P. Yakovlev, O.A. Nezhevenko, O.V. Danilov, D.G. Myakishev, and M.A. Tiunov, "State of the Art Simulations of Magnicon," AAC2002 Proceedings, Oxnard, June, 2002, AIP Conference Proc. 647, Woodbury, N.Y., 2002, pp. 421-432.
24. V.P. Yakovlev, O.A. Nezhevenko, J.L. Hirshfield, M.A. LaPointe, M.A. Batzova, G.I. Kuznetsov, "100 MW Electron Gun For A 34.3 GHz Magnicon," *Proceeding of 2001 Particle Accelerator Conference*, Chicago, June 17-22, 2001, pp.1041-104.